J. Limnol., 59(2): 156-166, 2000

Inland dissolved salt chemistry: statistical evaluation of bivariate and ternary diagram models for surface and subsurface waters

Robert M. BACA[1)]* and Stephen T. THRELKELD

Department of Biology, University of Mississippi, University MS 38677, USA
[1)]U.S. Environmental Protection Agency, 960 College Station Road, Athens, GA 30605, USA
*e-mail corresponding author: baca.robert@epa.gov

ABSTRACT

We compared the use of ternary and bivariate diagrams to distinguish the effects of atmospheric precipitation, rock weathering, and evaporation on inland surface and subsurface water chemistry. The three processes could not be statistically differentiated using bivariate models even if large water bodies were evaluated separate from small water bodies. Atmospheric precipitation effects were identified using ternary diagrams in water with total dissolved salts (TDS) <25 mg l^{-1} dominated by SO_4^{-2}, Ca^{+2}, and ($Na^+ + K^+$), though water whose inorganic chemistry was dominated by atmospheric precipitation were few. Waters affected by weathering had TDS of 15 to 1,000 mg l^{-1} and were dominated by ($HCO_3^- + CO_3^{-2}$) and Ca^{+2}. The effects of rock weathering on ion chemistry were the dominant mechanism influencing water chemistry. The contribution of silicates, carbonates, and evaporites to ions in weathering were distinguished using ternary diagrams. Weathering of silicates was evident in low TDS waters, while weathering of carbonates and evaporites was evident in moderate and high TDS waters, respectively. Evaporation effects were first obvious in water around 1,000 mg l^{-1} TDS as a shift towards higher SO_4^{-2}, Cl^-, and ($Na^+ + K^+$). At higher TDS, Cl^- became the dominant anion while ($Na^+ + K^+$) remained the dominant cation. The general patterns were consistent in lakes, rivers, and subsurface water bodies, although subsurface waters did not show an influence due to ions from atmospheric precipitation. While several of the TDS size classes separated statistically into distinct groups, there was wide variation in the pattern of inorganic ions within a TDS size class, especially when TDS >1000 mg l^{-1}. A principal components analysis showed that the variability in the relative proportions of the major ions was related to atmospheric precipitation, weathering, and evaporation. About half of the variation in the distribution of inorganic ions was related to rock weathering. By considering most of the important inorganic ions, ternary diagrams are able to distinguish the contributions of atmospheric precipitation, rock weathering, and evaporation to inland water chemistry.

Key words: inorganic ion chemistry, Gibbs model

1. INTRODUCTION

Gibbs (1970) attempted to predict the contributions of atmospheric precipitation, rock weathering, and evaporation to global inland water chemistry using a plot of total dissolved salts (TDS) against Na^+:($Na^+ + Ca^{+2}$) or Cl^-:($Cl^- + HCO_3^-$). This bivariate model predicted that water with low TDS and high Na^+ and Cl^- had chemistry dominated by atmospheric precipitation, water with moderate TDS and high Ca^{+2} and HCO_3^- by rock weathering, and water with high TDS and high Na^+ and Cl^- by evaporation.

The model proved to be controversial, as it was unable to accurately distinguish these three factors affecting water chemistry. Feth (1971) described how the bivariate model could not differentiate between salt spring inputs and evaporation. The data of Stallard & Edmond (1983) from the Amazon basin had high TDS and high Na^+ from the dissolution of evaporites rather than evaporation. Stallard & Edmond (1983) identified other water bodies whose chemistry was the result of the weathering of highly eroded siliceous rocks which the bivariate model predicted to be the result of atmospheric precipitation. Kilham (1990) presented data from intertropical Africa which deviated from the model due to cyclic salts, calcium carbonate precipitation, and dissolution of ancient salt. The dilute lakes of Eilers et al. (1992) plotted outside the bivariate model because of low weathering rates and the inability of the model to consider ions other than Na^+ and Ca^{+2}. In spite of this disagreement with the bivariate model, it is often retained as the null model against which to compare regional water chemistry (Armengol *et al*. 1991; Eilers *et al*. 1992; Gibson *et al*. 1995). It serves as a paradigm in several textbooks (Berner & Berner 1987, 1996; Comín & Williams 1994; Allan 1995; Langmuir 1997; Faure 1998) even though a few note the model as being controversial (Berner & Berner 1996; Langmuir 1997; Faure 1998).

We believe that the bivariate model fails to predict the influences of atmospheric precipitation, rock weathering, and evaporation on inland water chemistry because it does not consider enough of the major inorganic ions. Here we examine the bivariate model using a global set of data and present an alternate model using ternary diagrams which take into account most of the major inorganic ions in water. The bivariate model is evaluated statistically for the first time, as well as the ternary model. We compare the chemistry of lakes, rivers, and subsurface waters to assess the validity of the ternary model.

2. METHODS

Atmospheric precipitation data were obtained from Gorham (1961), Likens *et al*. (1970), Pearson & Fisher (1971), Stallard & Edmond (1981), Galloway *et al*. (1982), Meybeck (1983), and Dayan *et al*. (1985). These sources were used since several provided data on HCO_3^-, which is generally not reported for atmospheric precipitation. Data for lakes were obtained from Whitehead & Feth (1961), Livingstone (1963), Eugster & Hardie (1978), the Eastern and Western Lakes Surveys (Kanciruk *et al*. 1986; Eilers *et al*. 1987), Banens (1987), and Kling *et al*. (1992). River data were obtained from Livingstone (1963), Likens *et al*. (1970), Briggs & Ficke (1978), and Kling *et al*. (1992). Livingstone (1963) provided the data originally used by Gibbs (1970), but had relatively few concentrated or dilute water bodies. Whitehead & Feth (1961), Briggs & Ficke (1978), and Eugster & Hardie (1978) provided data on saline waters, while the Eastern and Western Lake Surveys, Likens *et al*. (1970), and Briggs & Ficke (1978) provided data on dilute waters. Banens (1987) and Kling *et al*. (1992) were added to the data to examine regional influences on ions. Subsurface water information came from White *et al*. (1963). Duplicate points cited in multiple papers were reduced to the original citation. All data were converted into units of mg l^{-1}, and no correction was made for cyclic salts. Total dissolved salts (TDS) was calculated as the sum of Na^+, K^+, Ca^{+2}, Mg^{+2}, Cl^-, SO_4^{-2}, HCO_3^-, and CO_3^{-2} in mg l^{-1}. Data were used only if values were reported for all of the major ions, so that values of 0 mg l^{-1} were measured values (except for CO_3^{-2} which was assumed to be negligible in low TDS waters if no value was reported). Because the Eastern and Western Lake Surveys were very large, they were sampled by randomly taking at least 20 lakes from each of the sub-regions and alkalinity classes listed by the authors.

The resulting data set contained 70 points for atmospheric precipitation, 646 rivers, 1369 lakes, and 280 subsurface waters. The data set was global in that there were samples from every continent except Antarctica, but were not uniformly distributed from around the world. Samples from the United States comprised 58% of the groundwater samples, 73% of the river samples, and 88% of the lake samples. The data set was not designed to be a probability sample of the range and average TDS values of inland waters around the globe. Rather it was developed to investigate the model of Gibbs (1970) and its data from Livingstone (1963), the concerns of Eilers *et al*. (1992) and Gibbs (1992) regarding dilute waters, the concerns of Feth (1971) and Kilham (1990) regarding concentrated waters, and the concern of Gibbs (1970, 1992) regarding major versus minor water bodies. This resulted in the use of several different published data sets so as to obtain a large number of samples to address the concerns listed above and discussed later. The patterns that we observed in the data set are intended to describe general processes rather than address specific populations of water bodies. Our data set as used in this paper is available on the internet (http://www.olemiss.edu/projects/iondata), and contains information on the name and location of the water bodies.

Bivariate plots were constructed using the format of Gibbs (1970) for cations and anions using only the data from lakes and rivers. Gibbs (1970) did not evaluate atmospheric precipitation or subsurface water, and were not plotted here. To evaluate the contribution of major water bodies to the model, we identified the largest lakes by surface area and the largest rivers by average annual discharge. If not included in the original citation, surface area and drainage information were obtained from Murray (1910), Hutchinson (1957), Encyclopaedia Britannica (1994), and Leopold (1994). Major rivers (n=167) were those with average annual discharges >9 km^3 y^{-1}. Major lakes (n=57) were those with surface areas >10 km^2.

Ternary diagrams were generated using data for atmospheric precipitation, lakes, rivers, and subsurface waters, which plot the relative proportion of three components of some mixture, in this case the major anions or cations. Anions were a mixture of SO_4^{-2}, Cl^-, and (HCO_3^- + CO_3^{-2}), while cations were represented by Ca^{+2}, Mg^{+2}, and (Na^+ + K^+). We chose these particular ions because they are often used in geochemical analyses (Hem 1985) and comprise most of the major inorganic ions in atmospheric precipitation (Gorham 1961; Carroll 1962; Pearson & Fisher 1971; Berner & Berner 1987), rock weathering (Rodhe 1949; Hutchinson 1957), and evaporation/crystallization (Hutchinson 1957; Eugster & Hardie 1978).

The type of rock weathering was examined with a ternary diagram using axes of Si (μmol l^{-1}), (HCO_3^- + CO_3^{-2}), and (SO_4^{-2} + Cl^-) (both sets in μeq l^{-1}). These axes were similar to those used by Stallard & Edmond (1982) and Ming-hui *et al*. (1982) for determining the contribution of silicates, carbonates, and evaporites during weathering. (HCO_3^- + CO_3^{-2}) was substituted for alkalinity because the latter was not available in all of the original data sets, and it provided the most comparable measurement.

To observe how the distribution of cations and anions in ternary diagrams changed with TDS, the data set was separated into TDS size classes. Ten size classes were chosen based on where changes in the proportions of ions were expected to occur (Hutchinson 1957) and also to show apparent patterns in the data. The size classes were 1-5, >5-15, >15-25, >25-50, >50-100, >100-500, >500-10^3, >10^3-10^4, >10^4-10^5, and >10^5 to 4x10^5 mg l^{-1} TDS.

The use of the bivariate and ternary models to distinguish TDS size classes was evaluated using an ANOVA followed by Student-Newman-Keuls *post-hoc* tests, all at $P \leq 0.01$. Proportional data used in the analy-

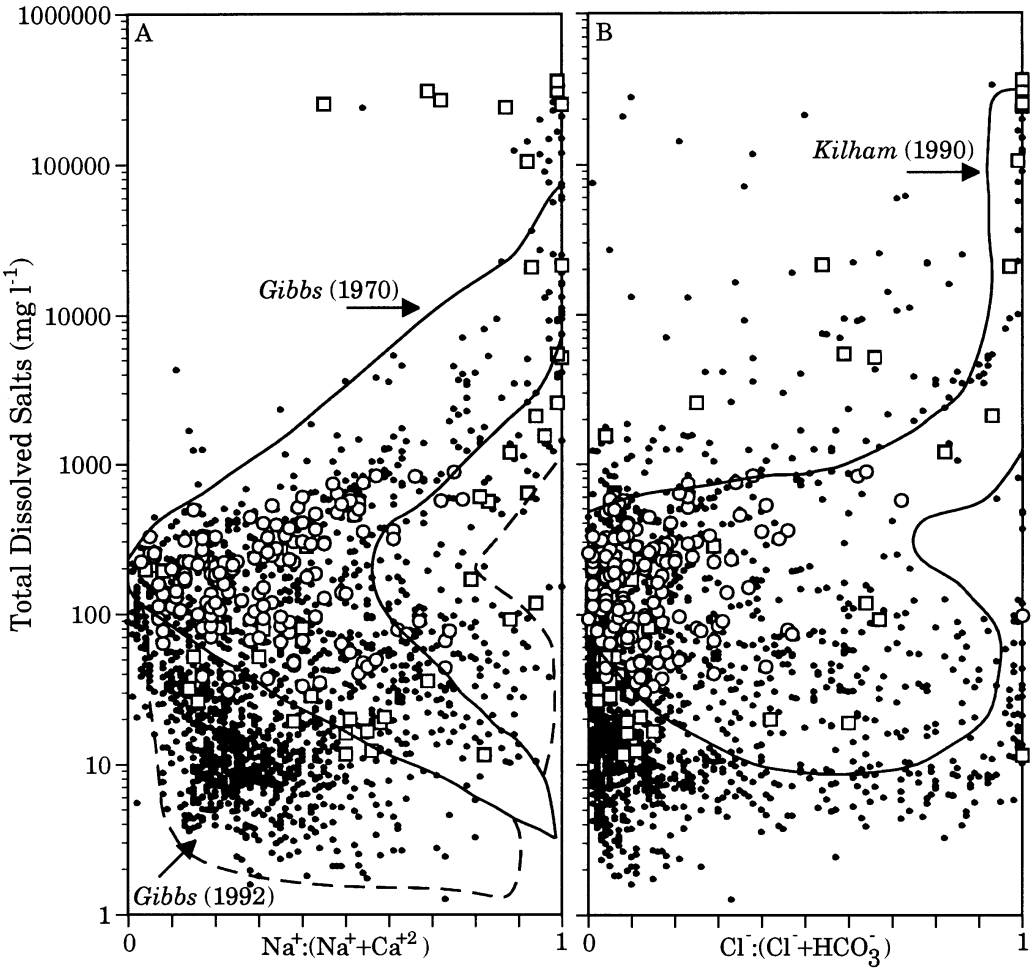

Fig. 1. Bivariate models of cations and anions overlaid with the shapes of the models of Gibbs (1970) (**solid line in A**), Gibbs (1992) (**dashed line in A**), and Kilham (1990) (**solid line in B**). These shapes apply to both the distribution of cations and anions, but are separated for clarity. Open circles indicate major rivers, open squares are major lakes, and closed circles are minor rivers and lakes as defined in the text.

ses were not transformed because the transformations did not greatly change the outcomes of the analyses, probably due to the large sample sizes. With little change in the outcome of the analyses, we felt that interpretation of the raw data rather than the transformed values would be easier to understand. Principal components analysis was performed on the data using the cationic proportions of Ca^{+2}, Mg^{+2}, and (Na^{+} + K^{+}) and the anionic proportions of SO_4^{-2}, Cl^{-}, and (HCO_3^{-} + CO_3^{-2}) as variables to determine the relationships among the ions, independent of the concentration of the ions. Factor loadings ≥|0.40| were considered of practical significance and used in interpretation of the components (Stevens 1992). All analyses were performed using SAS 6.03 (SAS Institute 1988).

3. RESULTS

The bivariate model plots for lakes and rivers did not show the boomerang or retort shapes found by Gibbs (1970) or Kilham (1990) (Fig. 1). Only the modified bivariate model (Gibbs 1992) fit the cation-ratio data to any extent, but failed to predict the anion-ratio data. In the Gibbs (1970, 1992) and Kilham (1990) models, the shapes were supposed to predict the distribution of both the cation- and anion-ratio plots, which they were not able to do. When only the major lakes and rivers were considered, there was still no agreement with the original model (Gibbs 1970). Several major lakes and rivers fell completely outside of the original models in both the cation and anion plots (Fig. 1). The ANOVA and Student-Newman-Keuls (SNK) *post-hoc* tests using Na^{+}:(Na^{+} + Ca^{+2}) or Cl^{-}:(Cl^{-} + HCO_3^{-}) as dependent variables against an independent variable of the TDS size classes indicated that the bivariate plots do not show the distinct groupings expected by the models (Fig. 2). Neither model distinguished any size class ≤250 mg l^{-1} TDS as significantly different from the others, whether the complete data set was used or only major waters considered.

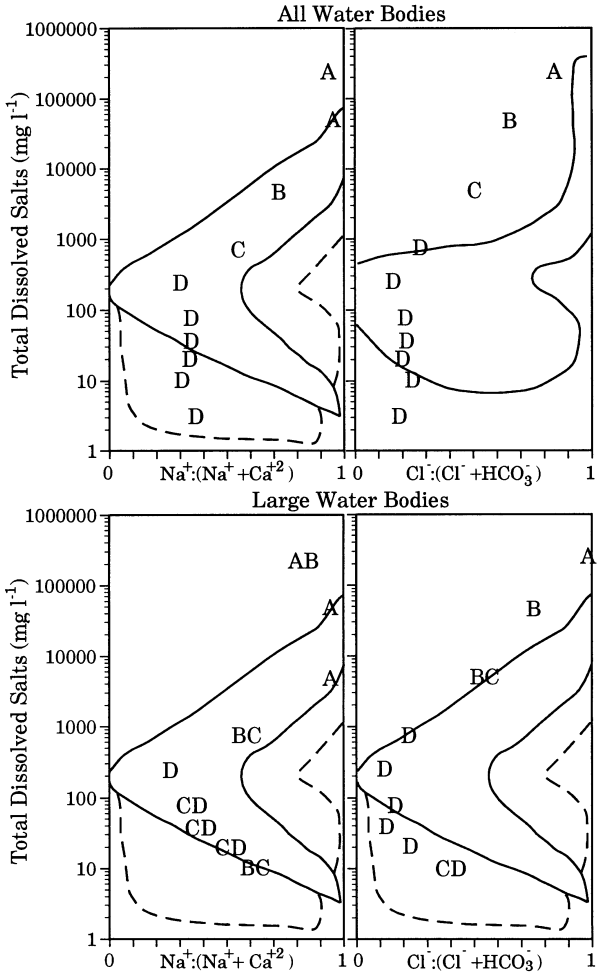

Fig. 2. Averages of TDS size classes and statistical groupings according to bivariate diagram plots. Averages are plotted as letters indicating the Student-Newman-Keuls *post-hoc* groupings. Different letters indicate significant differences between TDS size classes at $P \leq 0.01$. The upper figures are for all lake and river data, the lower figures for large lakes and rivers as defined in the text. Multiple letters indicate that a size class fell into more than one *post-hoc* group.

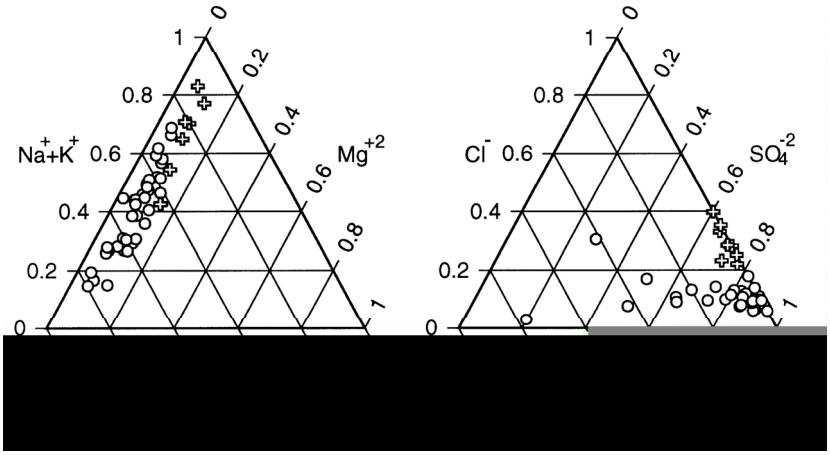

Fig. 3. Ternary diagrams of cations and anions for atmospheric precipitation. Proportions are based on data in mg l^{-1}. The orientation of the gridlines and axis values should be used to interpret the diagrams. Coastal precipitation (<100 km from coast) is shown as crosses, continental precipitation as circles.

Atmospheric precipitation always had <20% Mg^{+2} in cations and usually >60% SO_4^{-2} in anions (all data are percentages of anions or cations) (Fig. 3). Coastal precipitation (<100 km from the coast) had >40% (Na^+ + K^+), almost no (HCO_3^- + CO_3^{-2}), and higher Cl^- proportions than continental precipitation. Continental precipitation ranged from almost 90% Ca^{+2} to 92% (Na^+ + K^+) and had a wide range of (HCO_3^- + CO_3^{-2}) values, probably due to the variable pH in rain (3.0-9.8 worldwide [Carroll 1962]), aerosols, and blown dust. Precipitation had a TDS average and standard deviation of 12.5±26.3 mg l^{-1}, with values ranging from 0.3-175 mg l^{-1}.

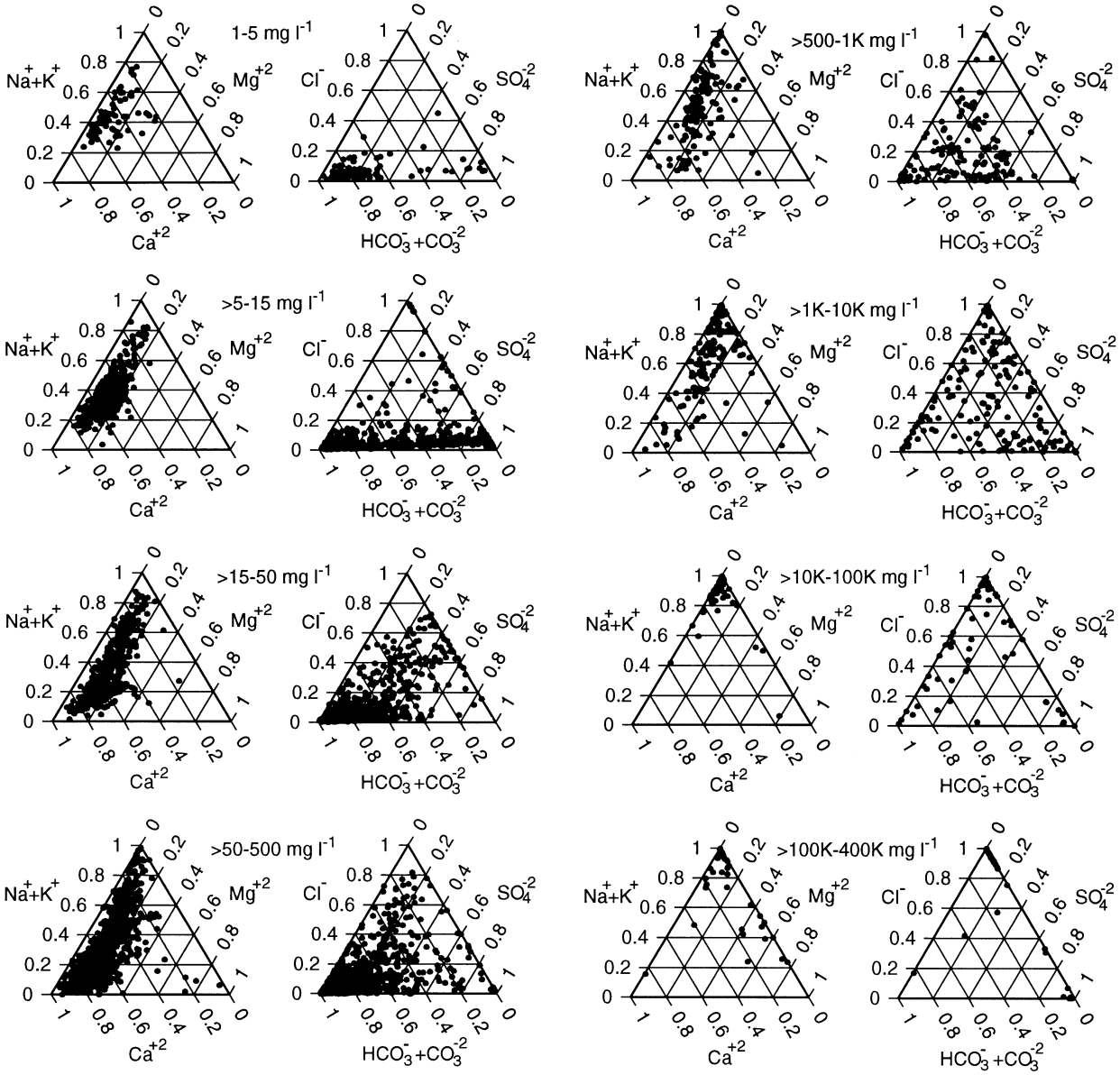

Fig. 4. Ternary diagrams of cations and anions from the same set of data as in figure 1 with the addition of subsurface waters. Proportions are based on data in mg l^{-1}. TDS size classes are labeled between pairs of ternary diagrams.

The most dilute surface waters (1-15 mg l^{-1} TDS) had a small set of cations that fell in the same area as precipitation which were high in SO_4^{-2} and low in both Cl^- and (HCO_3^- + CO_3^{-2}) (Figs 3 and 4). Most of the remaining points plotted high in (HCO_3^- + CO_3^{-2}). Cations were similar to that of precipitation, although there was a slight enrichment of Mg^{+2}. In water of 15-500 mg l^{-1} TDS, a large portion of the points were dominated by (HCO_3^- + CO_3^{-2}) (>60% of anions). SO_4^{-2} decreased in proportion to the other anions from typically >60% to often <30%. At TDS >500 mg l^{-1}, the proportions of both Ca^{+2} and (HCO_3^- + CO_3^{-2}) decreased. Anions shifted away from (HCO_3^- + CO_3^{-2}) dominance with a progression to SO_4^{-2} and Cl^- dominated brines as TDS increased. The proportion of Mg^{+2} in cations increased in the highest TDS size class as predicted by Hutchinson (1957).

To visualize if lakes, rivers, and subsurface waters differed in their ionic shifts with changes in TDS, we plotted the average proportion of individual ions in a TDS size class (not concentration which would bias towards the high end of a size class) separated into the three types of water body (Fig. 5). In cations, all waters showed little change along the Mg^{+2} axis. As water increased in TDS, cations first decreased and then increased in the proportion of (Na^+ + K^+), the latter which was in the direction of the average cation distribution for the open ocean (Meybeck 1983). Cation trends were

similar in all three water bodies in that changes occurred in the same direction and at the same TDS concentrations.

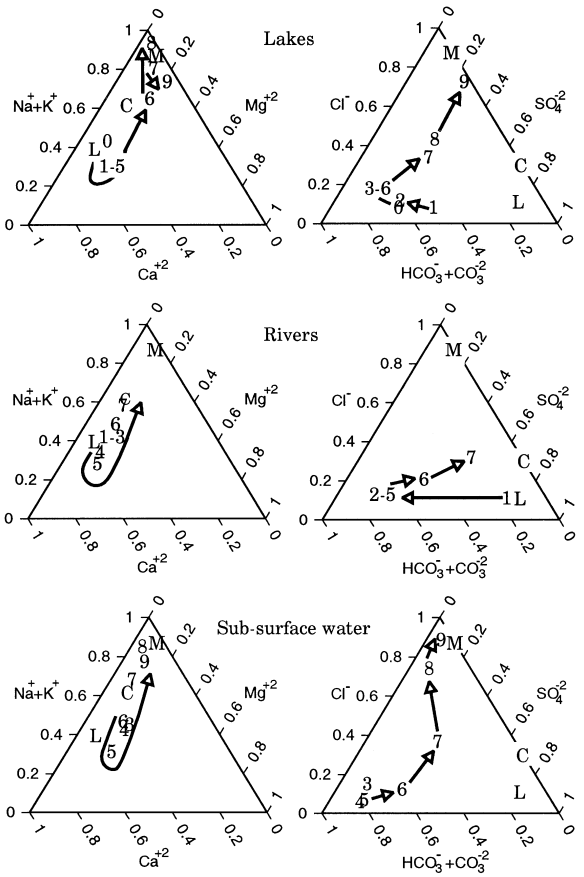

Fig. 5. Ternary diagrams of cations and anions for lakes, rivers, and subsurface waters showing the average proportions for the size classes. Figure labels are: L=continental precipitation, C=coastal precipitation, M=ocean water. TDS size classes are: 0=1-5 mg l^{-1}, 1=>5-15 mg l^{-1}, 2=>15-25 mg l^{-1}, 3=>25-50 mg l^{-1}, 4=>50-100 mg l^{-1}, 5=>100-500 mg l^{-1}, 6=>500-1,000 mg l^{-1}, 7=>1,000-10,000 mg l^{-1}, 8=>10,000-100,000 mg l^{-1}, 9=>100,000-400,000 mg l^{-1}. Rivers do not have a 1-5 mg l^{-1} size class and subsurface waters do not have size classes for 1-25 mg l^{-1}. Arrows indicate the general change in ionic proportions as TDS increases.

This similarity of changes in ionic proportions was also true for anions (Fig. 5). The lowest size classes of lakes and rivers plotted on a trajectory from atmospheric precipitation (high SO_4^{-2}) to high (HCO_3^- + CO_3^{-2}). Subsurface waters do not receive direct precipitation inputs, had TDS >25 mg l^{-1}, and showed their first size class with high (HCO_3^- + CO_3^{-2}). Three subsurface sites had TDS between 11-25 mg l^{-1}, but were not included due to the small sample size and their similarity to middle size classes as all three had >55% (Na^+ + K^+) and >65% (HCO_3^- + CO_3^{-2}). With further increases in TDS, all three types of water body displayed a decrease in (HCO_3^- + CO_3^{-2}), and an increase in SO_4^{-2} and Cl^-. The most concentrated waters became dominated on average by only Cl^-, except for rivers whose highest TDS value was <3% that for lakes and groundwater.

Statistical evaluation of differences among the size classes using all of the ions simultaneously was done using principal components analysis (PCA) and ANOVA. PCA was run for the data set of the proportions of cations and anions. The eigenvectors of the first principal component were entered as coefficients to generate a component score for each sample in the data set. This created a single value for every sample that was used as the dependent variable in an ANOVA followed by an SNK *post-hoc* ($P \leq 0.01$) with the TDS size classes as the independent variables (which were not part of the PCA). Significant differences in the variation of the proportions of cations and anions are shown in figure 6. TDS size classes that were not significantly different from each other are encircled. ANOVAs of the second and third principal components conducted as above separated the size classes into different groups, but are not presented because these groups were less distinct since the latter components explained less of the variation in the data (Tab. 1). The average component scores for each TDS size class from the PCA are examined in figure 7. The first three principal components explained 92% of the variation in the proportions of anions and cations (Tab. 1). An average component score for atmospheric precipitation data was plotted to aid in interpretation of the loadings.

The type of rock weathering was examined by plotting the size class averages in a ternary diagrams using axes of Si (µmol l^{-1}), (HCO_3^- + CO_3^{-2}), and (SO_4^{-2} + Cl^-) (both in µeq l^{-1}) (Fig. 8). Size class averages are shown for lakes and rivers combined and subsurface waters alone.

4. DISCUSSION

The bivariate models did not have the resolution needed to predict the effects of atmospheric precipitation, rock weathering, and evaporation/crystallization. Although the modified bivariate model of Gibbs (1992) encompassed most of the Na^+:(Na^+ + Ca^{+2}) data, it was extremely difficult to distinguish any processes in these plots (Fig. 1). While a model of global water chemistry will understandably have variability within it, too many factors blend together in the modified Gibbs model for it to be of much predictive value. No bivariate model was able to accurately predict the distribution of Cl^-:(Cl^- + HCO_3^-) data.

One of the factors thought to explain the inconsistency between the Gibbs (1970) model and data presented by other researchers which plotted outside the model is that the disparate points were from minor water bodies. Even when only major water bodies (defined here by discharge or surface area since no definition was presented in Gibbs [1970, 1992]) were considered, the original model was not supported well (Figs 1

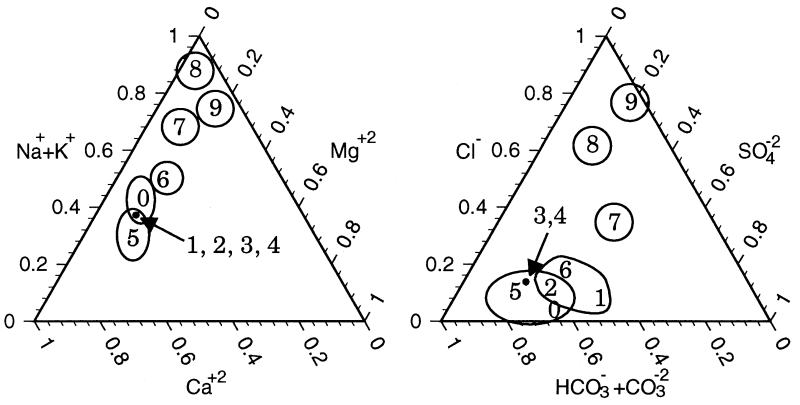

Fig. 6. Ternary diagrams indicating differences between TDS size class groupings. Size class averages for the entire data set are plotted as in figure 5. TDS size classes not significantly different (P>0.01) are encircled. Note that a size class can belong in multiple groups. Solid dots represent overlapping size classes.

Tab. 1. Principal components analysis showing component loadings of ions in lakes, rivers, subsurface waters, and atmospheric precipitation. Percent labels refer to that ion as a percent of (Na^{+}+K^{+}+Ca^{+2}+Mg^{+2}) or (Cl^{-}+SO_4^{-2}+HCO_3^{-}+ CO_3^{-2}). Significant loadings are shown in bold.

	Component 1	Component 2	Component 3
% variance explained	51.1	25.7	14.9
% Ca^{+2}	**0.497**	0.082	**-0.410**
% Mg^{+2}	0.231	0.295	**0.880**
% (Na^{+} + K^{+})	**-0.531**	-0.181	0.051
% Cl^{-}	**-0.484**	-0.146	0.069
% (HCO_3^{-} + CO_3^{-2})	**0.421**	**-0.509**	0.108
% SO_4^{-2}	-0.080	**0.770**	-0.196

and 2). Considering that one of our data sources was Livingstone (1963), the same used by Gibbs (1970), it is surprising that we could not reproduce or improve on Gibbs' model for major water bodies. At a minimum, TDS size class averages for major waters should plot within the original model. Although major waters showed somewhat more statistical separation in the lower TDS size classes, many of the averages fell outside the original model, especially in the anion data (Fig. 2). Small (1989) showed that as lake size increased, the variation in the concentration of Mg^{+2}, Ca^{+2}, and conductivity decreased. This means that in the bivariate model, data from small water bodies should be spread throughout and around the boomerang but have an average within the boomerang, which is not the case (Fig. 2). Sullivan *et al*. (1990) cautioned that relationships between water chemistry and lake size are probably only regional and are modified by various watershed and in-lake processes. The bivariate models failed because atmospheric precipitation and evaporation are not dominated by only Na^{+} and Cl^{-}, and rock weathering involves more ions than Ca^{+2} and HCO_3^{-} (Stallard & Edmond 1983; Banens 1987; Kilham 1990; Eilers *et al*. 1992).

Using ternary diagrams, we were able to distinguish the contributions of atmospheric precipitation, rock weathering, and evaporation to water chemistry. Atmospheric precipitation was dominated by SO_4^{-2} (>60%) which originates from both natural and anthropogenic sources (Meybeck 1983; Berner & Berner 1987), and this same signal in some of the very low TDS waters suggests that their chemistry was dominated by atmospheric inputs. Such unmodified atmospheric inputs were evident in only a small number of the lakes (<10%) and rivers (<1%) examined, indicating that atmospheric inputs were quickly modified by rock weathering. Since precipitation-dominated waters were uncommon even in low TDS waters (either through sampling bias or in reality), neither the bivariate nor ternary diagrams found statistically different groupings as a result of atmospheric precipitation (Figs 2 and 6). But only the ternary diagrams could show dilute waters high in SO_4^{-2} (Fig. 4, 1-15 mg l^{-1} TDS) resulting from atmospheric inputs.

Atmospheric precipitation had a TDS average of 12.5 mg l^{-1} which will concentrate 2.2x on average due to evaporation in the watershed before entering a stream (Berner & Berner 1987), meaning that precipitation effects should be evident in waters with TDS of ≤28 mg l^{-1} (although the concentration factor is estimated to range between 1.9x and 3.6x [Berner & Berner 1987] and TDS in precipitation was reported as high as 176 mg l^{-1} [Meybeck 1983]). This was true for lakes and rivers, but subsurface water did not show a precipitation signal in any data (Fig. 5). The streams that exhibited precipitation dominance in our data set were from the

un- and pre-treated Hubbard Brook watersheds and plotted very close to the average precipitation values found there (90% SO_4^{-2}, 10% Cl^-, 0% HCO_3^- in anions and 9% Mg^{+2}, 50% Ca^{+2}, and 41% ($Na^+ + K^+$) in cations [Likens *et al*. 1970]). The concentration of the dissolved ions in the streams at Hubbard Brook was 2.7x higher than that found in the precipitation, which was close to the estimated North American concentration factor of 2.6x (Berner & Berner 1987). The similarity of their proportions means that the stream water was mainly the result of atmospheric precipitation and loss of rain water to evaporation which caused the ions to concentrate.

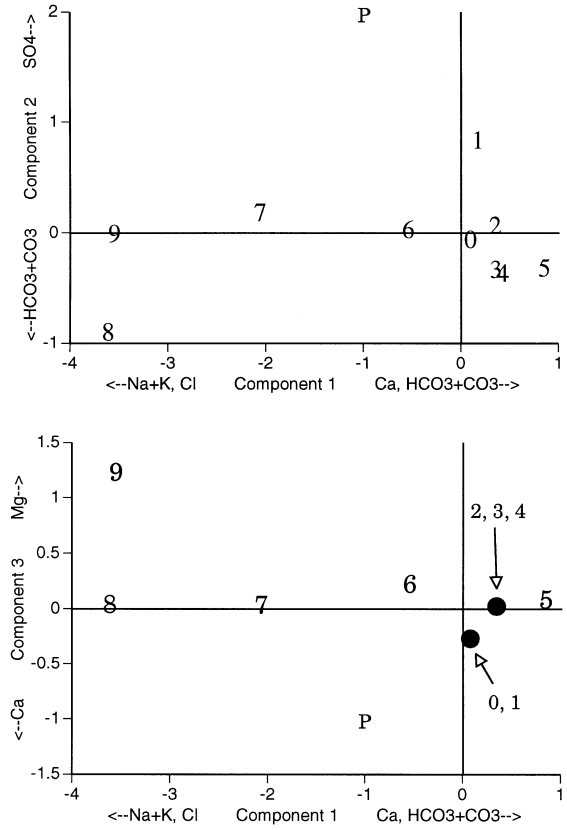

Fig. 7. The average principal component scores for the TDS size classes and atmospheric precipitation. Size class labels are given in figure 5. The component averages for atmospheric precipitation are labeled P. Closed circles represent overlapping size classes. Axes were labeled according to the significant component loadings given in table 1.

But more often in dilute lakes and rivers the ionic proportions of rain water were modified by the surrounding watershed before it entered the lake or river. This effect was observed in parts of the Amazon basin (Stallard & Edmond 1983), Cascades-Sierra Nevadas, Minnesota, and Wisconsin (Eilers *et al*. 1992) where the low weathering rates made it difficult to separate the effects of precipitation and rock weathering. Even in the low TDS size classes (≤25 mg l^{-1}) where precipitation-dominance was expected, most lakes and rivers showed a high proportion of ($HCO_3^- + CO_3^{-2}$) and Ca^{+2} indicative of rock weathering, and statistically separated into multiple overlapping groups suggesting a blurring of atmospheric precipitation and weathering effects (Fig. 6). Pearson & Fisher (1971) compared the precipitation load to the stream load of ions in a few moderately sized watersheds (<190 km^2). While the percentages of SO_4^{-2} and Cl^- in the streams were almost equal to that in the precipitation, Ca^{+2}, Mg^{+2}, and ($Na^+ + K^+$) were often 2 to 3x higher in the stream than in the precipitation, showing how the watershed can modify the ionic concentration and proportions of rain before it enters a lake or river. In two small watersheds (<11 km^2), Katz *et al*. (1985) found that although nearly all of the sulfate in streams was due to dry deposition, less than 20% of the total dissolved load was from atmospheric precipitation, with the rest due to weathering.

As solutes increased in concentration, ($HCO_3^- + CO_3^{-2}$) increased in proportion due to rock weathering, as did Ca^{+2} but to a lesser extent. Waters in basins composed of limestone, dolomite, shale, sandstone, acid igneous rocks, or metamorphic rocks all have relatively high HCO_3^- (Eugster & Hardie 1978). Rock weathering effects were observed in TDS size classes ranging from 25-500 mg l^{-1}, with average ionic proportions falling in areas on the ternary diagrams predicted for weathering by Rodhe (1949) and Hutchinson (1957). It not surprising that this TDS range included 48% of the data, as freshwater is considered bicarbonate in general (Rodhe 1949; Hutchinson 1957).

Weathering effects throughout the entire range of TDS values were confirmed in figure 8. According to Stallard & Edmond (1982), weathering of silicates causes points to fall near the silica vertex, weathering of carbonates plots near the alkalinity (here $HCO_3^- + CO_3^{-2}$) vertex, and weathering of evaporites near the ($SO_4^{-2} + Cl^-$) vertex. Low TDS waters fell closest to the silica vertex. Meybeck (1983) estimated the SiO_2 content of rain to be 0.3 mg l^{-1}, and such a low value in rain indicates that the relatively high silica signal in these dilute waters was most likely due to silicate weathering. This was supported by the similar trends between the low TDS subsurface waters which do not receive direct atmospheric precipitation and the low TDS lakes and rivers. The 100-500 mg l^{-1} TDS size class showed the highest contribution due to carbonate weathering. The highest size classes showed a dominance along the ($Cl^- + SO_4^{-2}$) axis, indicating a mix of weathering of evaporites and evaporation/crystallization. Weathering of evaporites was confirmed in the data from subsurface waters, which are not susceptible to the effects of evaporation (although samples taken at the surface of thermal springs will probably be affected by evaporation if the water is boiling). The trends shown in figure 8 were similar to that of Stallard & Edmond (1982) and Berner & Berner (1996), although the averages for lakes and rivers are shifted towards

(SO_4^{-2} + Cl^-) compared to Stallard & Edmond (1982) because we could not correct for cyclic salts.

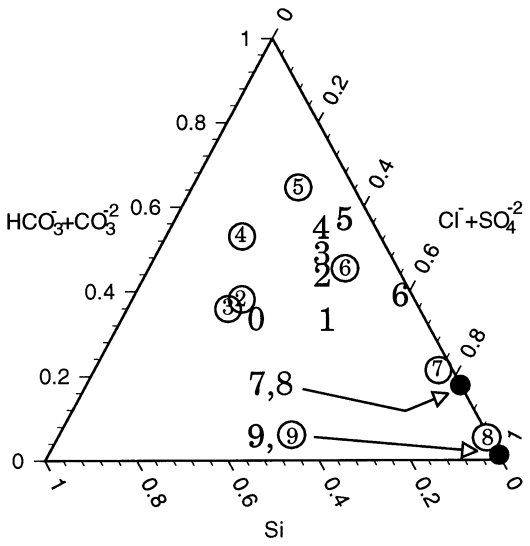

Fig. 8. Ternary diagram showing the effect of various underlying rocks in the weathering process. Labels are the TDS size classes given in figure 5. Data from lakes, rivers, and subsurface waters were in µmol l^{-1} for Si and µeq l^{-1} for (Cl^- + SO_4^{-2}) and (HCO_3^- + CO_3^{-2}). Circled numbers are averages from subsurface waters, large numbers are averages from lakes and rivers combined. Closed circles represent overlapping size classes.

As with Stallard & Edmond (1982), the pattern in figure 8 appears to be related to the susceptibility of various rocks to weathering. Quartz (SiO_2) and K-feldspar ($KAlSi_3O_8$) are resistant to weathering and will contribute to low TDS and high SiO_2 water when weathered. Calcite ($CaCO_3$) and dolomite ($CaMg(CO_3)_2$) are moderately susceptible to weathering and will contribute to moderate TDS and high HCO_3^- to water. Halite (NaCl), gypsum ($CaSO_4 \cdot 2H_2O$), and anhydrite ($CaSO_4$) are highly susceptible to weathering and will contribute to high TDS and high Cl^- or SO_4^{-2} to water (Feth 1971; Stallard & Edmond 1982; Berner & Berner 1987). These mechanisms contrast the bivariate models (Gibbs 1970; 1992) which suggest that the lowest TDS water are controlled by atmospheric precipitation and the highest TDS waters by evaporation.

Although it was difficult to separate the effects of evaporite weathering from evaporation in figures 5 and 8, the changes in the ion concentrations indicate that evaporation was also occurring. This mechanism can be inferred because the changes in ions corresponded to the changes that would occur based on the expected order that various salts precipitate out of solution, and that most of the very high TDS data in lakes and rivers came from endorheic basins. The first to precipitate on average is calcite, which can be seen in the 500-10^3 mg l^{-1} TDS size class with a decrease in the proportion of both Ca^{+2} and (HCO_3^- + CO_3^{-2}), although the waters remain a bicarbonate brine (Fig. 4) (Clarke 1924; Hutchinson 1957; Eugster & Hardie 1978). Further increases in TDS (10^3-10^4 mg l^{-1}) shifted waters to a combination of SO_4^{-2}- and Cl^--dominated brines as dolomite precipitates. At even higher TDS values, gypsum and anhydrite will come out of solution, removing SO_4^{-2} and Ca^{+2}, resulting in Cl^-- and Na^+- dominated waters (Clarke 1924; Hutchinson 1957; Eugster & Hardie 1978). This is only a general trend which explains the average patterns shown in figure 5, and is similar to average trends in brine evolution presented by Hutchinson (1957) and Hardie & Eugster (1970).

Other pathways in the evolution of brines exist which will vary based on the particular concentrations of ions before precipitation begins (Hardie & Eugster 1970; Faure 1998). Garrels & Mackenzie (1967) presented a pathway in which calcite precipitates first, followed by sepiolite ($Mg_2Si_3O_8 \cdot nH_2O$) and amorphous silica (SiO_2). SO_4^{-2} does not come out of solution because Ca^{+2} was depleted by the precipitation of calcite, and the brine becomes concentrated in Na^+, K^+, Cl^-, and SO_4^{-2}. Hardie & Eugster (1970) built upon this model and presented several more pathways which include brines dominated by (Na^+, Ca^{+2}, Mg^{+2}, Cl^-), (Na^+, Mg^{+2}, SO_4^{-2}, Cl^-), and (Mg^{+2}, Ca^{+2}, Cl^-). These alternative pathways of brine evolution explain the wide variation in ions seen in figure 4 at TDS > 1000 mg l^{-1}, as even small differences in the initial composition of the water can produce very different brines (Faure 1998).

Although it appears that rivers did not become as concentrated in TDS as lakes and groundwater (Fig. 5), this was likely due to sampling bias. Rivers and streams were defined as flowing water on the surface, and while highly concentrated flowing waters exist at least as outflows from salt springs and saline lakes, it is likely that they were of very low flow or intermittent flow and were not measured by our sources of data. In this data set, the highest reported TDS value for rivers was 9,488 mg l^{-1} for the Brazos River in Texas as opposed to 361,076 mg l^{-1} TDS for Urmia Lake in Iran and 324,567 mg l^{-1} TDS for a test well in New Mexico.

The principal components analysis suggests that the changes in ionic proportions as TDS increased were the result of atmospheric precipitation, weathering, and evaporation. The first component loaded positive for Ca^{+2} and (HCO_3^- + CO_3^{-2}) and negative for (Na^+ + K^+) and Cl^-. The chemistry involved with these ions is the weathering of carbonates in the positive direction and the weathering of evaporites and evaporation in the negative direction. Since weathering was the most prevalent mechanism determining ion chemistry, it is likely that the first component, which explained the largest amount of the variation in the data (51%), is defined by weathering. The second component loaded positive for SO_4^{-2} and negative for (HCO_3^- + CO_3^{-2}), relating scores to the importance of SO_4^{-2} chemistry.

Positive scores in low TDS size classes indicated the contribution of atmospheric precipitation, the less positive scores in the higher TDS size classes related to SO_4^{-2} brines, and the negative scores related to carbonate chemistry. The third component was positive for Mg^{+2} and negative for Ca^{+2} which represents the stage of evaporation/crystallization. Ca^{+2} is the first to come out of solution during crystallization and high negative third component scores represent the early stages of evaporation. Mg^{+2} only changes in the ternary diagrams as a result of the later stages of evaporation, and high positive component scores represent the later stages of evaporation. The gradients explained by the second and third components are not as clear as the first, due to them explaining less of the variation in the data.

There are several factors other than atmospheric precipitation, weathering, and evaporation that affect water chemistry. Distance from the ocean, pollution, regional climate, biota, and land use patterns all influence the type and concentration of ions in natural waters (Hutchinson 1957; Gorham 1961; Meybeck 1983; Berner & Berner 1987, 1996; Bluth & Kump 1994). Perhaps the most important factor is the underlying geology, which affects both the type and concentration of ions that get into solution, and has effects across the entire range of TDS (Eugster & Hardie 1978; Stallard & Edmond 1983; Berner & Berner 1987, 1996; Eilers *et al*. 1992; Faure 1998). Consideration of these factors in future analyses should further explain the variation in figure 4, and may show regional TDS patterns that are different from figure 5.

Despite the other mechanisms and variability within the data, the ternary diagram model was able to identify waters strongly influenced by atmospheric precipitation which were low in TDS (1-25 mg l^{-1}), plotted near the SO_4^{-2} vertex in anions, and plotted near 50% (Na^+ + K^+)-50% Ca^{+2} in cations. Waters strongly influenced by weathering processes were moderate in TDS (25-500 mg l^{-1}), and on average plotted near the Ca^{+2} and (HCO_3^- + CO_3^{-2}) vertices. When evaporation/crystallization influenced water chemistry, TDS was high (>1000 mg l^{-1}), anions plotted from near the 33:33:33% point to near the Cl^- vertex, and cations plotted between 60-100% (Na^+ + K^+). But as described above, the effect of weathering on water chemistry was detected in all size classes and can dominate the water chemistry of a region in any TDS size class. The evaporation process is quite variable and can cause samples to plot far from the average values shown in figures 5 and 6.

The strength of the ternary diagrams is that they add several more axes (one for each ion and one for TDS) in order to view complex changes in ion chemistry which cannot be observed with the bivariate model. The bivariate models fail because they are based on incorrect assumptions, and need to be removed as the paradigm for explaining inland water chemistry. Gibbs (1992) states, "Until a better model is devised, it seems practical to continue using the Gibbs model with some modifications." Ternary diagrams are a better model because they provide a more accurate method by which to predict and compare the regional- to global-scale contributions of atmospheric precipitation, rock weathering, and evaporation to water chemistry.

ACKNOWLEDGMENTS

We thank J. Washington, C. Ochs, B. Libman, G. Davidson, C. Cleveland, B. Cash, B. Brooks and several anonymous reviewers for helpful comments on the manuscript. We also thank the numerous others in the Biology Department at the University of Mississippi for their comments on early versions of the manuscript. R. Baca was partially supported by EPA R821832-01-0 and NSF DEB 9528840 to S. Threlkeld.

Disclaimer. This paper has been reviewed in accordance with the US Environmental Protection Agency's peer and administrative review policies and approved for publication. Mention of trade names or commercial products does not constitute endorsement or recommendation for use by the US EPA.

REFERENCES

Allan, J.D. 1995. *Stream ecology: structure and function of running waters*. Chapman and Hall, London: 388 pp.

Armengol, J., J. Catalán, N. Gabellone, D. Jamune, J. de Manuel, E. Martí, J.A. Morguí, J. Peñuelas, M. Real, J.L. Riera, S. Sabater, F. Sabater & J. Toja. 1990. A comparative limnological study of the Guadalhorce Reservoirs system (Málaga, S.E. Spain). *Scientia Ger*., 16: 27-41.

Banens, R.J. 1987. The geochemical character of upland water of northeast New South Wales. *Limnol. Oceanogr*., 32: 1291-1306.

Berner, E.K. & R.A. Berner. 1987. *The global water cycle*. Prentice-Hall, Englewood Cliffs: 397 pp.

Berner, E.K. & R.A. Berner. 1996. *Global environment: water, air, and geochemical cycles*. Prentice-Hall, Upper Saddle River: 376 pp.

Bluth, G.J.S. & L.R. Kump. 1994. Lithologic and climatologic controls of river chemistry. *Geochim. Cosmochim. Acta*, 58: 2341-2359.

Briggs, J.C. & J.F. Ficke. 1978. Quality of rivers of the United States, 1975 water year - based on the National Stream Quality Accounting Network (NASQAN). *USGS Open-File Report*, 78-200.

Carroll, D. 1962. Rainwater as a chemical agent of geologic processes-a review. *USGS Water-Supply Paper*, 1535-G.

Clarke, F.W. 1924. The data of geochemistry, fifth ed. *Bull. US Geol. Survey* 770.

Comín, F.A. & W.D. Williams. 1994. Parched continents: our common future? In: R. Margalef (Ed.), *Limnology now: a paradigm of planetary problems*. Elsevier Science, Amsterdam: 473-527.

Dayan, U., J.M. Miller, A.M. Yoshinaga & D.W. Nelson. 1985. An assessment of precipitation chemistry measurements from the global trends network and its predecessors (1972-1982). *NOAA Technical Memorandum*, ERL ARL-136.

Eilers, J.M., D.F. Brakke & A. Henriksen. 1992. The inapplicability of the Gibbs model of world water chemistry for dilute lakes. *Limnol. Oceanogr*., 37: 1335-1337.

Eilers, J.M., P. Kanciruk, R.A. McCord, W.S. Overton, L. Hook, D.J. Blick, D.F. Brakke, P.E. Kellar, M.S. DeHaan, M.E. Silverstein & D.H. Landers. 1987. Characteristics of

lakes in the western United States. 2. Data compendium for selected physical and chemical variables. *EPA*, 600/3-86/054b.
Encyclopaedia Britannica 1994. Micropaedia 7, 15th ed., Chicago.
Eugster, H.P. & L.A. Hardie. 1978. Saline lakes. In: A. Lerman (Ed), *Lakes: chemistry, geology, physics*. Springer-Verlag, New York: 237-293.
Faure, G. 1998. *Principles and applications of geochemistry*. Prentice-Hall, Upper Saddle River: 600 pp.
Feth, J.H. 1971. Mechanisms controlling world water chemistry: evaporation-crystallization process. *Science*, 172: 870-871.
Galloway, J.N., G.E. Likens, W.C. Keene & J.M. Miller. 1982. The composition of precipitation in remote areas of the world. *J. Geophys. Res*., 87: 8771-8786.
Garrels, R.M. & F.T. Mackenzie. 1967. Origin of the chemical composition of some springs and lakes. In: R.F. Gould (Ed), *Equilibrium concepts in natural water systems*. American Chemical Society, Washington DC: 222-242.
Gibbs, R.J. 1970. Mechanisms controlling world water chemistry. *Science*, 170: 1088-1090.
Gibbs, R.J. 1992. A reply to the comment of Eilers et al. *Limnol. Oceanogr*., 37: 1338-1339.
Gibson, C.E., Y. Wu, S.J. Smith & S.A. Wolfe-Murphy. 1995. Synoptic limnology of a diverse geological region: catchment and water chemistry. *Hydrobiologia*, 306: 213-227.
Gorham, E. 1961. Factors influencing supply of major ions to inland waters, with special reference to the atmosphere. *Bull. Geol. Soc. Am*., 72: 795-840.
Hardie, L.A. & H.P. Eugster. 1970. The evolution of closed-basin brines. *Mineral. Soc. Amer. Spec. Pap*., 3: 273-290.
Hem, J.D. 1985. Study and interpretation of the chemical characteristics of natural water. *USGS Water-Supply Paper*, 2254.
Hutchinson, G.E. 1957. *A treatise on limnology. I. geography, physics, and chemistry*. John Wiley and Sons, New York: 1015 pp.
Kanciruk, P., J.M. Eilers, R.A. McCord, D.H. Landers, D.F. Brakke & R.A. Linthurst. 1986. Characteristics of lakes in the eastern United States. 3. Data compendium of site characteristics and chemical variables. *EPA*, 600/4-86/007c.
Katz, B.G., O.P Bricker & M.M. Kennedy. 1985. Geochemical mass-balance relationships for selected ions in precipitation and stream water, Catoctin Mountains, Maryland. *Am. J. Sci*., 285: 931-962.
Kilham, P. 1990. Mechanisms controlling the chemical composition of lakes and rivers: Data from Africa. *Limnol. Oceanogr*., 35: 80-83.
Kling, G.W., W.J. O'Brien, M.C. Miller & A.E. Hershey. 1992. The biogeochemistry and zoogeography of lakes and rivers in arctic Alaska. *Hydrobiologia*, 240: 1-14.
Langmuir, D. 1997. *Aqueous environmental geochemistry*. Prentice-Hall, Upper Saddle River: 600 pp.

Received: March 2000
Accepted: September 2000

Leopold, L.B. 1994. A view of the river. Harvard University Press, Cambridge: 298 pp.
Likens, G.E., F.H. Bormann, N.M. Johnson, D.W. Fisher & R.S. Pierce. 1970. Effects of forest cutting and herbicide treatment on nutrient budgets in the Hubbard Brook watershed-ecosystem. *Ecol. Monogr*., 40: 23-47.
Livingstone, D.A. 1963. Chemical composition of rivers and lakes. *USGS Professional Paper*, 440-G.
Meybeck, M. 1983. Atmospheric inputs and river transport of dissolved substances. *Int. Assoc. Hydrol. Sci. Publ*., 141: 173-192.
Ming-hui, H., R.F Stallard & J.M. Edmond. 1982. Major ion chemistry of some large Chinese rivers. *Nature*, 298: 550-553.
Murray, J. 1910. The characteristics of lakes in general, and their distribution over the surface of the globe. In: J. Murray & L. Pullar (Eds), *Bathymetrical survey of the Scottish fresh-water lochs*. Challenger, Edinburgh: 514-658.
Pearson, F.J., Jr. & D.W. Fisher. 1971. Chemical composition of atmospheric precipitation in the northeastern United States. *USGS Water-Supply Paper*, 1535-P.
Rodhe, W. 1949. The ionic composition of lake waters. *Verh. int. Ver. Limnol*., 10: 377-386
SAS Institute. 1988. *SAS/STAT User's Guide, 6.03*. SAS Institute, Cary: 1028 pp.
Small, M.J. 1989. Regional distributions of water quality derived as averages of spatial random processes. In: S. Ragone (Ed), *Regional characterization of water quality*. IAHS Pub., 182: 3-10.
Stallard, R.F. & J.M. Edmond. 1981. Geochemistry of the Amazon. 1. Precipitation chemistry and the marine contribution to the dissolved load at the time of peak discharge. *J. Geophys. Res*., 86: 9844-9858.
Stallard, R.F. & J.M. Edmond. 1983. Geochemistry of the Amazon. 2. The influence of geology and weathering environment on the dissolved load. *J. Geophys. Res*., 88: 9671-9688.
Stevens, J. 1992. *Applied Multivariate Statistics for the Social Sciences, 2nd ed*. Lawrence Erlbaum Associates, Hillsdale: 629 pp.
Sullivan, T.J., D.L. Kugler, M.J. Small, C.B. Johnson, D.H. Landers, B.J. Rosenbaum, W.S. Overton, W.A. Krester & J. Gallagher. 1990. Variation in Adirondak, New York, lakewater chemistry as function of surface area. *Wat. Res. Bull.*, 26: 167-176.
White, D.E., J.D. Hem & G.A. Waring. 1963. Chemical composition of sub-surface waters. *USGS Professional Paper*, 440-F.
Whitehead, H.C. & J.H. Feth. 1961. Recent chemical analyses of waters from several closed-basin lakes and their tributaries in the western United States. *Bull. Geol. Soc. Am*., 72: 1421-1426.